Available online at www.sciencedirect.com

SCIENCE DIRECT®

Biomaterials 24 (2003) 4213–4221

Biomaterials

www.elsevier.com/locate/biomaterials

Degradation characteristics of hydroxyapatite coatings on orthopaedic TiAlV in simulated physiological media investigated by electrochemical impedance spectroscopy

Ricardo M. Souto[a,*], María M. Laz[b], Rui L. Reis[c]

[a] Department of Physical Chemistry, University of La Laguna, Campus de Anchieta, E-38071 La Laguna (Tenerife), Canary Islands, Spain
[b] Department of Edaphology and Geology, University of La Laguna, Campus de Anchieta, E-38071 La Laguna (Tenerife), Spain
[c] Department of Polymer Engineering, University of Minho, Campus de Gualtar, 4710-057 Braga, Portugal

Received 15 December 2002; accepted 13 May 2003

Abstract

This paper concentrates on the degradation characteristics of hydroxyapatite (HA) coatings on orthopaedic Ti–6Al–4V alloy while immersed in Ringer's salt solution, which were investigated by electrochemical impedance spectroscopy. Electrochemical impedance spectroscopy measurements were used to in situ characterize the electrochemical behavior of the passivated alloy covered with HA during aging in Ringer's solution. Comparison of the electrochemical data for the coated material with that for the uncoated metal substrate was also performed. The characteristic feature that describes the electrochemical behavior of the coated material is the coexistence of large areas of the coating itself with pores where the substrate is exposed to the aggressive media. The interpretation of results was thus performed in terms of a two-layer model of the film, in which the precipitation of hydrated oxide or phosphate compounds seals the pores left by the ceramic coating. The blocking effect due to salt precipitation inside the pores produces an enhancement of the resistance values, thus effectively diminishing the metal ion release in the system.

Keywords: Biomaterials; Hydroxyapatite; Ti–6Al–4V; Plasma-sprayed coatings; Corrosion resistance; Electrochemical impedance spectroscopy

1. Introduction

Metallic materials have found wide application in restorative surgery as basic biomaterials for manufacturing implant prostheses for skeletal replacements and fixtures. In this case, metallic materials which combine good mechanical characteristics, high corrosion resistance and good compatibility with biological materials are chosen. Amongst the various materials currently employed, the alloy Ti–6Al–4V has found extensive biomedical applications due to its good mechanical properties and ability for osseointegration [1], combined with an excellent corrosion behavior due to passivity. Passivity is due to the very stable and tenaciously adherent oxide films spontaneously formed over the surface [2–6], which reform very rapidly if removed or mechanically damaged. These films are fairly unreactive, though transient microscopic breakdown of the passive state induced by the presence of chloride ions in the environment has been recently observed in vitro [7,8]. When the prostheses are placed in the human body, the passive films undergo further transformations, namely thickening of the passivating film and stoichiometric changes, as well as metal dissolution [9–12]. Both passivation and metal dissolution are processes of an electrochemical nature.

Enhanced biocompatibility of titanium-base materials is achieved by coating them with ceramic biomaterials, and through this they have become the most widely used material combination for dental and orthopaedic implants [13,14]. The material response is governed by ion leaching and by corrosion with the release of particles. These processes are not only dependent on solubility (especially in the case of surface reactive

*Corresponding author. Tel.: +34-922-318030; fax: +34-922-318002.
E-mail addresses: rsouto@ull.es (R.M. Souto), mmlaz@ull.es (M.M. Laz), rgreis@dep.uminho.pt (R.L. Reis).

0142-9612/03/$ - see front matter © 2003 Elsevier Ltd. All rights reserved.
doi:10.1016/S0142-9612(03)00362-4

biomaterials, such as glasses, glass ceramics or calcium phosphate ceramics), but also on intercellular turnover, cellular activity, bacteria, pH, fretting due to biomechanical situation, electrochemical processes at the interface and other factors. They usually imply a change in the chemical composition and physical properties of the interface. In addition to it, the processes undergone at the buried interface between the metal and the ceramic or polymeric material must be known and characterized. Amongst the materials employed, hydroxyapatite (HA) coatings are specially attractive, as a bone-like material is introduced in the interface between the metal and the living tissue, which results in improved osseointegration [15–18]. The stability of these biomaterials still originate from their electrochemical passivity, and their ability to avoid passivity breakdown in the highly aggressive physiological environment. But at this stage, there is scarce information on the electrochemical behavior of ceramic coated biomaterials in the scientific literature.

This investigation was aimed to investigate the effect of plasma-sprayed HA-coatings on Ti–6Al–4V substrates regarding the corrosion behavior of the metallic biomaterials during experiments in physiological media. Electrochemical impedance spectroscopy (EIS) was the major investigative technique, since it has the potential to discover new information on the processes occurring, whilst not interfering significantly with the mechanisms operating. Based on the properties of the coating and the corrosion reaction at the coating/substrate interfaces, much more information can be collected than by routine DC electrochemical methods [19,20]. The spectra of bare and coated substrates were recorded, and the data were analyzed to evaluate the equivalent circuit parameters in each case with the goal of determining the degradation characteristics of ceramic-coated biomaterials.

2. Materials and methods

2.1. Materials

Ti–6Al–4V alloy matching the ASTM F136-84 was used as the substrate. Metal substrate was annealed at 750°C for 2 h, and air cooled. Then the substrate was alumina grit blasted to a surface roughness R_A (mean roughness, DIN 4762) = 1.66 μm and R_Z (roughness depth, DIN 4768) = 5.61 μm, and passivated in nitric acid. Some specimens were then coated with HA. HA-coatings with a thickness of 50 ± 10 μm on Ti–6Al–4V were produced by plasma spraying. Samples were beam shaped ($180 \times 30 \times 6\,mm^3$), and coatings performed by Plasma Biotal Company, Tideswell, UK.

2.2. Electrochemical test

The investigation of the corrosion characteristics of the HA-coatings deposited on Ti–6Al–4V substrates was studied by electrochemical methods. Testing was carried out in Ringer's physiological solution open to air, not stirred, at room temperature. The composition of the testing solution is presented in Table 1 [21]. The electrolyte was prepared with Millipore MilliQ* plus water (resistivity greater than 18 MΩ cm), and analytical grade reagents.

The electrochemical measurements were performed with a flat three-electrode cell, consisting of the studied sample, a saturated calomel electrode (SCE) employed as reference electrode, and a sufficiently large platinum grid as auxilliary electrode. The specimen area exposed to the electrolyte solution was $1\,cm^2$.

Polarization curves and electrochemical impedance spectra (EIS) measurements were determined by using an EG&G Princeton Applied Research model 283A potentiostat/galvanostat controlled from a computer. Prior to the beginning of the polarization procedures, the samples were kept in the solution for 55 min in order to establish the free corrosion potential (E_{cor}). The potentiodynamic polarization curves were obtained with a scan rate of 1 mV/s from −1000 mV (SCE). The measurement of the EIS was performed at the open circuit potential. A sine wave of 15 mV (rms) was applied across the cell at the open circuit potential of the system. The spectra were acquired in a 50 kHz–5 mHz frequency range by introducing an EG&G Princeton Applied Research model 5208 two-phase lock-in analyzer. A data density of six frequency points per decade was used, and spectra data were averaged over four cycles at each frequency. Impedance spectra were represented in both complex impedance diagram (Nyquist plot), and Bode amplitude and phase angle plots. In the Nyquist graph, the imaginary component of the impedance is plotted as a function of the real component, whereas the Bode representation shows the logarithm of the impedance modulus $|Z|$ and phase angle ϕ as a function of the logarithm of the frequency f. The analysis of the EIS was performed using a non-linear least squares fit method to obtain the equivalent electrical model for the substrate–electrolyte

Table 1
Composition of the simulated physiological solution: Ringer's balanced salt solution [21]

Compound	Ringer's solution concentration ($g\,dm^{-3}$)
NaCl	8.6
$CaCl_2$	0.48
KCl	0.3

interfaces after different exposure times in the testing solution.

3. Results

3.1. Polarization experiments

In order to compare the susceptibility to corrosion of the HA-coated specimen in relation to the bare alloy material, the anodic polarization potentiodynamic curves of the two materials in Ringer's physiological solution were first recorded. Prior to the beginning of the polarization procedures, the samples were kept in the solution for 55 min in order to establish the free corrosion potential (E_{cor}). Subsequently, the potentiodynamic polarization curves were obtained with a scan rate of 1 mV/s from −1000 mV (SCE). The measured polarization plots are depicted in Fig. 1.

From the inspection of the polarization curves, the onset of passivity is found to occur in the same potential region for both the coated and the uncoated specimens, thus indicating that formation of the oxide passive film apparently occurs under a similar mechanism and under similar potential requirements on them. In this way, after an initial range of cathodic depassivation, the open circuit potential is reached for the samples. An active–passive transition is observed next with passivating currents in the order of a few microamperes, which are typically observed during the passivation of titanium and its alloys [22]. Despite the reported similarities between the two systems, some differences can be observed when considering the potential dependence of the passive currents. Whereas a somewhat slow increase of the passivation current is observed for the uncoated specimen as the applied potential is made more positive, the HA-coated specimen shows an increase of this current for almost two orders of magnitude when the potential is set more positive than 1.5 V. This observation could be taken as an indication of an increased metal dissolution in the system through the passive film when the material is coated with hydroxyapatite, as it has been proposed by some authors [23,24]. But increased currents would also occur if the metal dissolves from the metallic substrate and precipitates as hydrated salts on the its surface [25,26], which has been claimed to result in enhanced corrosion resistance of the underlying metal substrate [26]. Conventional electrochemical techniques do not allow to distinguish between the two cases, and justifies the controversy existing in the scientific literature on whether enhanced or hindered metal ion release occurs for HA-coated Ti–6Al–4V substrates [23–26].

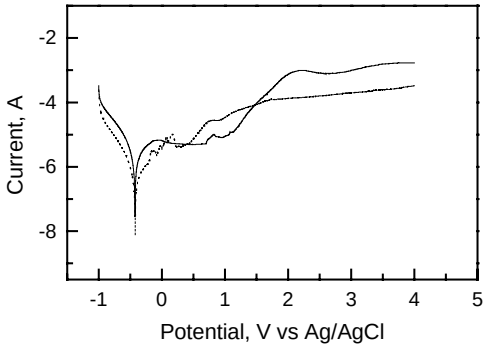

Fig. 1. Potentiodynamic polarization curves measured for (- - - - -) bare and (——) HA-coated Ti–6Al–4V alloy specimens after immersion in Ringer's solution.

3.2. Electrochemical impedance spectra

Electrochemical impedance experiments were performed at the open circuit potential. Typical examples of the impedance spectra obtained at different exposure times during the immersion in Ringer's simulated physiological solution of the HA-coated specimen are shown in Fig. 2. They are displayed in both complex impedance (Nyquist diagram), and Bode amplitude and phase angle plots. Though Nyquist plots are relatively featureless, the Bode plots are more indicated for the investigation of changes in the electrochemical characteristics of the system with aging. In this way, it was observed that upon immersion of the HA-coated specimen in the test electrolyte, variations in the impedance spectra occurred already during the first day of exposure, which resulted from the evolution of the electrochemical behavior of the system. Changes are less noticeable with time elapsing, and after 20 days exposure, an almost stationary behavior was reached. These observations clearly show that the electrochemical properties of the film change with exposure time.

The impedance spectra displayed in Fig. 2 exhibit two time constants at all exposure times. That is, they can be divided into two distinct frequency regions: the time constant in the high-frequency part, which arises from the uncompensated ohmic resistance due to the electrolytic solution and the impedance characteristics resulting from the penetration of the electrolyte through a porous film, and the low-frequency part accounting for the processes taking place at the substrate/electrolyte interface. Such a behavior is typical of a metallic material covered by a porous film which is exposed to an electrolytic environment, and can be described in terms of an equivalent circuit which accounts for the different electrochemical processes occurring in the system.

3.3. Selection of the equivalent circuit

For the interpretation of the electrochemical behavior of a system from EIS spectra, an appropriate physical model of the electrochemical reactions occurring on the

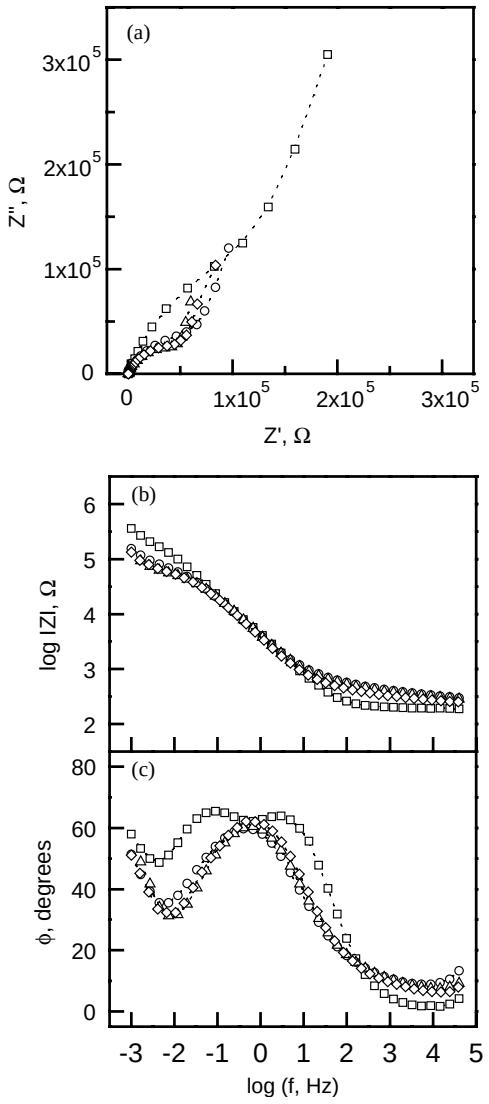

Fig. 2. Impedance spectra recorded for an HA-coated Ti–6Al–4V alloy specimen exposed to the Ringer's solution at diverse exposure times: (□) 2 hours; (○) 40 days; (△) 80 days; and (◇) 128 days.

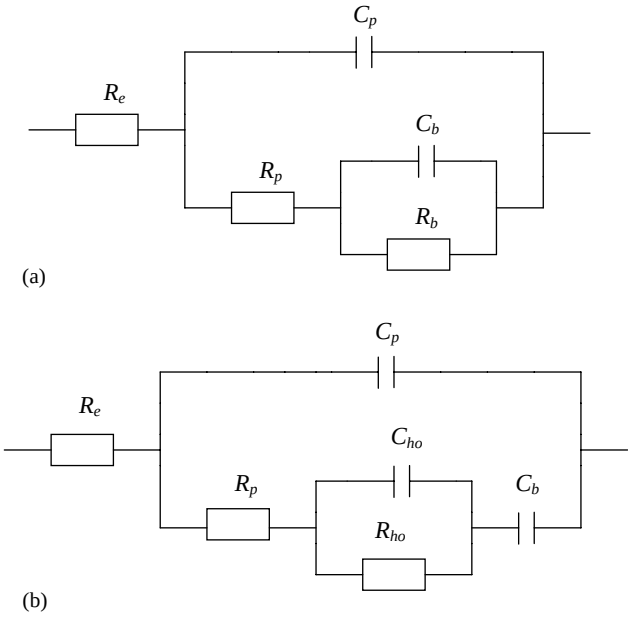

Fig. 3. Equivalent circuits used for the interpretation of the measured impedance spectra. (a) Two-layer model of an unsealed porous surface film; (b) two-layer model of a sealed porous surface film.

electrodes is necessary. The electrochemical cell, because it presents an impedance to a small sinusoidal excitation, may be represented by an equivalent circuit [27]. An equivalent circuit consists of various arrangements of resistances, capacitors and other circuit elements, and provides the most relevant corrosion parameters applicable to the substrate/electrolyte system.

After testing a number of different electrical circuit models in the analysis of the impedance spectra obtained at different exposure times, it was found that the whole set of data could be satisfactorily fitted with the two equivalent circuits given in Fig. 3. They are both based on the consideration of a two-layer model for the surface film. Circuit A was deduced to represent the electrochemical behavior of a metal covered with an unsealed porous film [28,29]. The equivalent circuit consists of the following elements: a solution resistance R_e of the test electrolyte, electrical leads, etc., the capacitance C_p of the intact (non-defective) coating layer, the charge transfer resistance associated with the penetration of the electrolyte through the pores or pinholes existing in the coating R_p, and the polarization resistance of the susbstrate R_b as well as the electrical double-layer capacitance at the substrate/electrolyte interface C_b.

On the other hand, circuit B was developed to represent a sealed anodic oxide film [30]. That is, the model represented by circuit A has been modified to take in account the precipitation of some hydrates/precipitates inside the surface porous film, thus hindering the penetration of the electrolyte to the metal substrate through the pores of the surface films. In this case, the components C_{ho} and R_{ho} introduced in circuit B represent the capacitance and resistance of hydrates/precipitates inside the pores of the surface film.

A reasonable fit to the equivalent circuit for a given impedance spectra was established by admitting a relative error [31] of less than 1% for the real and imaginary parts of the impedance. Next, the quality of fitting was judged by the error distribution vs. the frequency comparing experimental with simulated data for different models. This procedure is illustrated in Figs. 4 and 5 which show the experimental and simulated spectra for two exposure times, as well as the corresponding error distributions after the application of circuits A and B, respectively. Inspection of these figures show that both circuits satisfy the first of the criteria, with errors of less than 1% in all cases. But the comparison of the simulated and experimental spectra

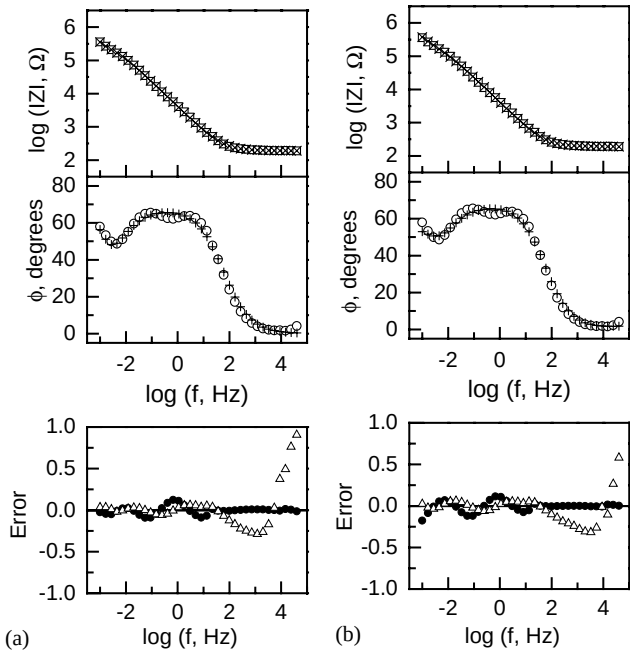

Fig. 4. Comparison of fitting quality of the two equivalent circuits given in Fig. 3. Bode plots (upper diagrams) and relative error (lower diagrams) for HA-coated specimen after 2 h exposure to Ringer's solution. Left figures (a): fitting with circuit A; right figures (b): fitting with circuit B. Key for $|Z|$: (□) experiment; (×) simulation. For ϕ: (○) experiment; (+) simulation. For relative errors: (●) real; (△) imaginary.

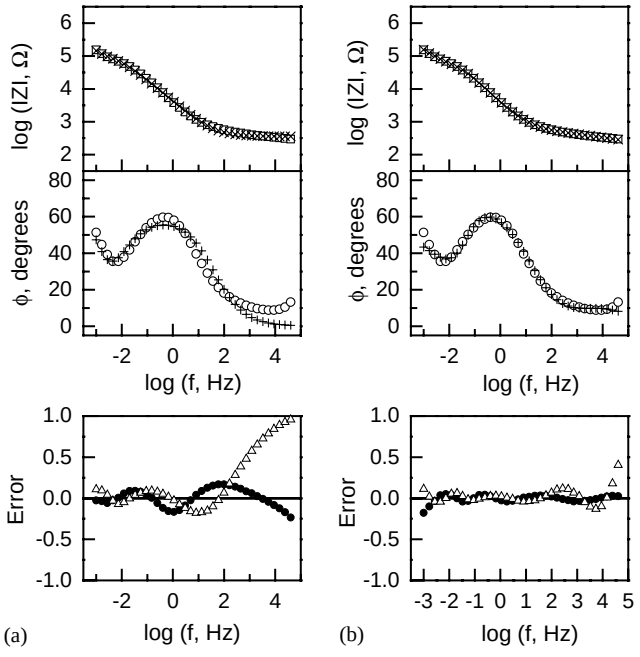

Fig. 5. Comparison of fitting quality of the two equivalent circuits given in Fig. 3. Bode plots (upper diagrams) and relative error (lower diagrams) for HA-coated specimen after 40 days exposure to Ringer's solution. Left figures (a): fitting with circuit A; right figures (b): fitting with circuit B. Key for $|Z|$: (□) experiment; (×) simulation. For ϕ: (○) experiment; (+) simulation. For relative errors: (●) real; (△) imaginary.

show that the best results are always attained by employing circuit B. A special mention must be made about early exposure times, such as those given in Fig. 4 for the spectra measured after 2 h exposure to the physiological solution. In this case, both circuits provide similar distributions over the frequency range studied.

Thus, when HA-coated Ti–6Al–4V alloy is exposed to Ringer's solution, its EIS spectra exhibit behavior typical of a porous film on the metallic substrate. Electrolyte penetration occurs through the pores of the ceramic coating, thus exposing the underlying metal to the physiological environment. But EIS spectra demonstrate an evolution with elapsed time that reflects that progressively the pores in the coatings are filled with precipitates, and after ca. 20 days exposure, these precipitates quite effectively seal the pores. Nevertheless, the blockage of the pores in the coating by precipitates do not result in an effective blockage of the metal. That is, no effective blockage is provided by the salts deposited in the pores, and metal dissolution continues through the coating. This conclusion is sustained by the fact that resistance values in the impedance spectra are below $10^6\,\Omega\,cm^2$ at all exposure times.

Such an observation is confirmed by the time dependency of the fitted parameters R_{ho} and C_{ho} (cf. Fig. 6), which represent the effects due to the precipitation of salts in the pores of the coating. Major variations are observed during within 20 days from the time the specimen was exposed to the solution, but a rather stationary condition is achieved after that time. This is an indication that the metal substrate achieves an

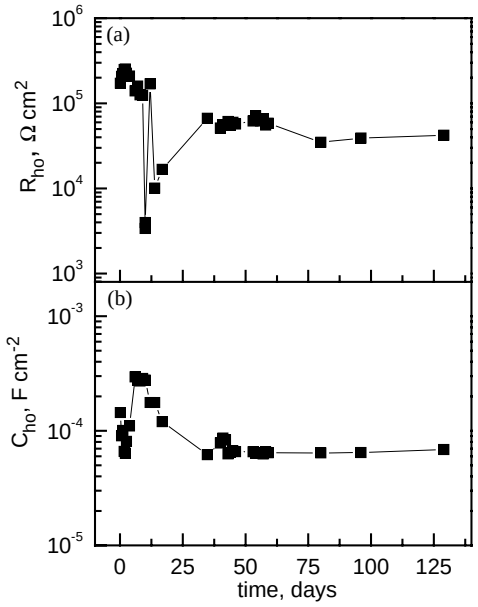

Fig. 6. Evolution of parameters (a) hydrated precipitate resistance inside pores, R_{ho}, and (b) hydrated precipitate capacitance, C_{ho}, with immersion time, determined from the fits of the impedance spectra to circuit B.

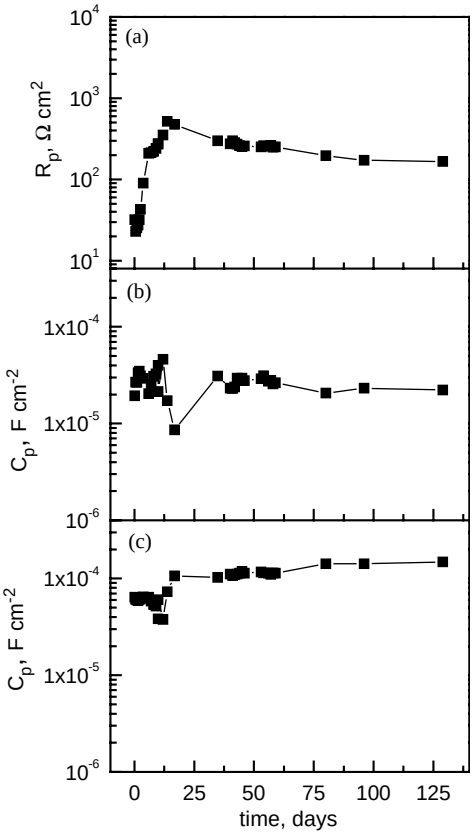

Fig. 7. Evolution of parameters (a) electrolytic solution resistance inside pores, R_p, and (b) porous layer capacitance, C_p, and (c) barrier layer capacitance, C_b, with immersion time, determined from the fits of the impedance spectra to circuit B.

approximately constant rate of dissolution when immersed in Ringer's solution.

The effect of precipitates partially blocking the conductive ionic paths in the pores after 20 days can also be observed from the inspection of the values of R_p as plotted in Fig. 7a, which give the electrolytic solution resistance inside the pores. As a result of the progressive blocking effect due to salt precipitation inside the pores in the ceramic coating, a significant and stable growth of R_p values is observed in time until they reach a stationary value after 20 days. No further variation of the resistance R_p was observed during the remaining part of the experiment. On the other hand, no significant variations were observed for C_p and C_b, respectively, the porous layer and the barrier layer capacitances, during the complete time interval covered by our experiments (cf. Figs. 7b and c). Thus, it can be concluded that the variations in the electrochemical system are related to changes in the chemical environment inside the pores existing in the HA-coating.

Finally, it must be noticed that the elements represented in both circuits as capacitors C_b and C_p were fitted as constant phase elements. This is a general diffusion related to element Q which accounts for deviations from ideal dielectric behavior related to surface inhomogeneities [32] or current leakage in the interface. Thus, a dissipation factor (n) is associated with them. This element is written in its admittance form as

$$Y^*(\omega) = Y_0(j\omega)^n,$$

where Y_0 is the adjustable parameter used in the non-linear least-squares fitting, and n is defined as the phenomenological coefficient which can be obtained from the slope of $|Z|$ on the Bode plot [33]. Pure capacitance behavior is represented by $n = 1.0$. In Fig. 8, the time dependencies of n values for both elements are shown. The low n values indicate a rough surface of the coating film, and these values may even increase with the time elapsed since immersion of the specimen in the physiological solution.

3.4. Comparative remarks

Comparison of the HA-coated specimen in relation to the bare alloy material was also performed on the basis of the measured EIS, as shown in Fig. 9. In this case, the substrate was employed as received, without any further pre-treatment. Under these conditions, the Ti–6Al–4V alloy is covered by a passive oxide film that has been spontaneously developed during exposure to air. This oxide layer is typically in the order of some tens of nanometers, and its electrochemical impedance characteristics could also be described in terms of the model circuit A. This observation agrees well with the previous findings by Pan et al. [34–36] derived from the EIS spectra measured for titanium samples immersed in biofluids with and without H_2O_2. In this case, the double-layer titanium oxide film was hypothesized to consist of a Ti–TiO_2 inner-TiO_2 outer porous unsealed layer when titanium was immersed in physiological solution without H_2O_2 [34,35], or in H_2O_2-containing biofluid at short exposure times [36], and to evolve into a Ti–TiO_2 inner-TiO_2 outer porous sealed layer when

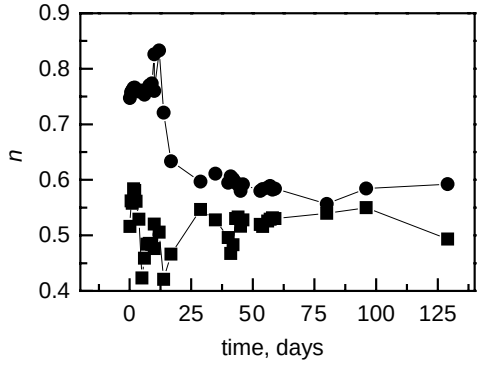

Fig. 8. Evolution of coefficient n for the various constant phase elements as calculated from the application of circuit B. (■) values refer to C_p; (●) values refer to C_b.

titanium was immersed in the H_2O_2-containing medium at longer exposures [36], in which case model circuit B was applicable instead.

Differences can be observed from the inspection of the EIS spectra depicted in Fig. 9, which were measured for both systems after a 1 h immersion in Ringer's solution. The spectra were subsequently analyzed, and could be satisfactorily modeled in terms of the model circuit A. The resulting impedance parameters are given in Table 2. From their comparison it can be observed that a significant increase of the resistance values for the HA-coated system, which are two orders of magnitude higher for R_p and R_b than those determined for the bare metal. In this way, though the HA-coating is not an effective anticorrosion layer, it hinders to some extent the electrochemical processes occurring at the metal substrate interface, thus contributing to a decrease in the metal ion release from the system.

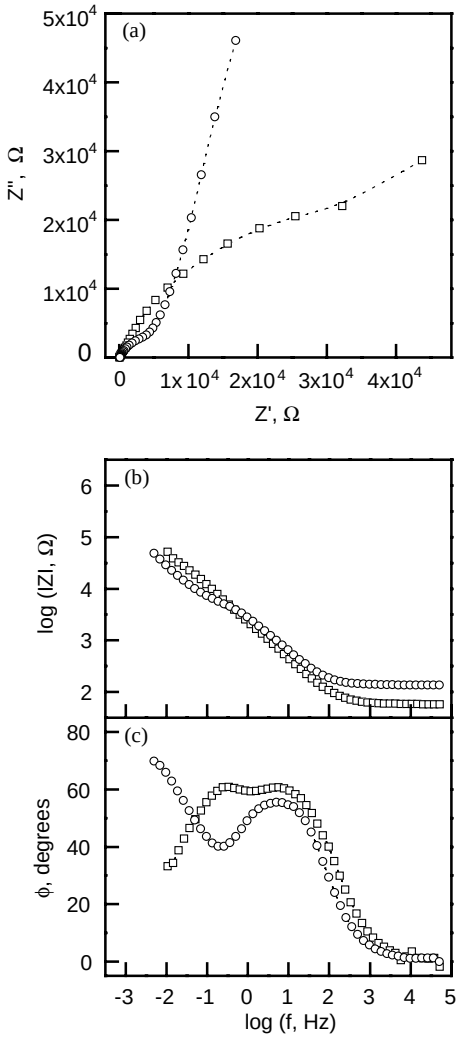

Fig. 9. Impedance spectra recorded for (□) an HA-coated Ti–6Al–4V alloy specimen, and for (○) a bare Ti–6Al–4V alloy sample, after exposure to the Ringer's solution for 2 h.

4. Conclusions

- Electrochemical impedance spectroscopy is a very useful technique for studying the corrosion behavior of surgical implant alloys, even when they are coated with a ceramic material such as hydroxyapatite.
- Over the frequency range applied the equivalent circuit employed for the description of the coated samples provides the best fitting of the experimental data. Two-layer models satisfactorily describe the electrochemical behavior of the system by considering a porous film on the metallic substrate. Metal dissolution occurs through the pores in the HA-coating, and leads to the precipitation of salts which block the pores. The resulting precipitates layer originates an additional barrier to metal dissolution in the system, as it can be followed through a significant increase in the resistance values measured after ca. 20 days. Nevertheless, it should be realized that this barrier does not provide an effective protection against metal dissolution, as there is only a reduction in its extent. The nature of the salts was not investigated in this study, but may probably be the result of metal phosphate formation or incorporation of metal ions in the HA structure [25].
- The electrochemical behavior of the system is characterized by the dissolution and passivation characteristics of the underlying metallic substrate. In this way, similar spectra are measured for both coated and uncoated substrates despite the obvious major differences existing in the physical characteristics of both systems. That is, the bare alloy relies on the formation of a porous oxide film for the achievement of the passive state, and the thickness of such layer is typically in the order of a few tens of nanometer. On the other hand, the HA-coating layer

Table 2
Impedance parameters of uncoated and HA-coated Ti6Al4V samples after immersion in Ringer's balanced salt solution for 1 h

Specimen	C_p (F cm^{-2})	n_p	R_p (Ω cm^2)	C_b (F cm^{-2})	n_b	R_b (Ω cm^2)
Uncoated	1.27×10^{-4}	0.777	5.11×10^3	6.47×10^{-5}	0.74	6.25×10^4
HA-coated	6.20×10^{-5}	0.751	4.59×10^5	4.26×10^{-4}	1.00	2.44×10^6

Impedance spectra have been fitted with model circuit A [28,29].

investigated ranged 50–200 μm and was very porous in nature. Despite these thickness values were ca. 1000 times bigger than those expected for an oxide passive layer, a two-layer model of the surface film accurately describes the electrochemical behavior of the coated system. That is, the corrosion resistance of the biomaterial is not greatly affected by the presence of the ceramic coating, but rather depends on the passivation ability of the metallic substrate and, to a minor extent, on the porosity of the ceramic coating.

- After a 4 month exposure to Ringer's solution, no evidence was found from the EIS that might indicate a (partial) detachment of the HA film from the underlying alloy. Thus, it can be expected that the coated system may outstand longer exposure periods in this physiological solution.

Acknowledgements

This work was initiated within the framework of a Collaborative Research Programme (Acción Integrada No. HP1995-0092 and HP1996-0109) between Spain and Portugal. Support for work conducted at the University of La Laguna by the Ministerio de Ciencia y Tecnología (Spain) under contract BQU2000-0867 is gratefully acknowledged.

References

[1] Albrektsson T, Branemark P-I, Hansson HA, Kasemo B, Larsson K, Lundstrom I, McQueen DH, Skalak R. The interface zone of inorganic implants in vivo—titanium implants in bone. Ann Biomed Eng 1983;11:1–27.

[2] Solar RJ. Corrosion resistance of titanium surgical implant alloys: a review. In: Syrett SC, Acharya A, editors. Corrosion and degradation of implant materials. Philadelphia: ASTM Special Technical Publication STP 684; 1979. p. 259–72.

[3] Ask M, Lausmaa J, Kasemo B. Preparation and surface spectroscopic characterization of oxide-films on Ti6A14V. Appl Surf Sci 1989;35:283–301.

[4] Johansson C, Lausmaa J, Ask M, Hansson H-A, Albrektsson T. Ultrastructural differences of the interface zone between bone and Ti6Al4V or commercially pure titanium. J Biomed Eng 1989;11:3–8.

[5] Lausmaa J, Kasemo B, Mattson H, Odelius H. Multitechnique surface characterization of oxide-films on electropolished and anodically oxidized titanium. Appl Surf Sci 1990;45:189–200.

[6] Reis RL, Paiva OC, Santos JD. Potentiostatic controlled growth of a very stable titanium oxide anodic film on Ti–6Al–4V alloy. Bioceramics 1994;7:125–30.

[7] Souto RM, Burstein GT. A preliminary investigation into the microscopic depassivation of passive titanium implant materials in vitro. J Mater Sci: Mater Med 1996;7:337–43.

[8] Souto RM, Burstein GT. Study of corrosion processes with electrochemical noise measurements. Mater Sci Forum 1998;289–292:799–806.

[9] Ducheyne P, Willems G, Martens M, Helsen J. Invivo metal-ion release from porous titanium-fiber material. J Biomed Mater Res 1984;18:293–308.

[10] Sundgren J-E, Bodo P, Lundstrom I. Auger-electron spectroscopic studies of the interface between human-tissue and implants of titanium and stainless-steel. J Colloid Interf Sci 1986;110:9–20.

[11] Healy KE, Ducheyne P. Oxidation-kinetics of titanium thin-films in model physiological environments. J Colloid Interf Sci 1992;150:404–17.

[12] Healy KE, Ducheyne P. The mechanisms of passive dissolution of titanium in a model physiological environment. J Biomed Mater Res 1992;26:319–38.

[13] de Groot K, Geesink R, Klein CPAT, Serekian P. Plasma sprayed coatings of hydroxyapatite. J Biomed Mater Res 1984;21:1375–87.

[14] Brown S. The medical physiological potential of plasma-sprayed ceramic coatings. Thin Solid Films 1984;119:127–39.

[15] Klein CPAT, Patka P, Wolke JGC, de Blieck-Hogevorst JMA, de Groot K. Long-term in-vivo study of plasma-sprayed coatings on titanium-alloys of tetracalcium phosphate, hydroxyapatite and alpha-tricalcium phosphate. Biomaterials 1994;15:146–50.

[16] Moroni A, Caja VL, Sabato C, Egger EL, Gottsauner-Wolf F, Chao E. Bone ingrowth analysis and interface evaluation of hydroxyapatite coated versus uncoated porous titanium porous bone implants. J Mater Sci: Mater Med 1994;5:411–6.

[17] Tisdel CL, Goldberg VM, Parr JA, Bensusan JS, Staikoff LS, Stevenson S. The influence of a hydroxyapatite and tricalcium-phosphate coating on bone growth into titanium fiber-metal implants. J Bone Joint Surg 1994;76A:159–71.

[18] Tranquilli PL, Merolli A, Palmacci O, Gabbi G, Cacchioli A, Gonizzi G. Evaluation of different preparations of plasma-spray hydroxyapatite coating on titanium-alloy and duplex stainless-steel in the rabbit. J Mater Sci: Mater Med 1994;5:345–9.

[19] Bundy KJ, Dillard J, Luedemann R. Use of a.c. impedance methods to study the corrosion behaviour of implant alloys. Biomaterials 1993;14:529–36.

[20] Mansfeld F, Lee CC, Kovacs P. Application of electrochemical impedance spectroscopy (EIS) to the evaluation of the corrosion behavior of implant materials. Proc Electrochem Soc 1994;94–15:59–72.

[21] Gluszek J, Masalski J. The influence of variations in pH of Ringer's solution on corrosion behaviour of surgical steel. In: Costa JM, Mercer AD, editors. Progress in the understanding and prevention of corrosion. London: Institute of Materials; 1993. p. 1289–96.

[22] Burstein GT, Souto RM. Observations of localised instability of passive titanium in chloride solution. Electrochim Acta 1995;40:1881–8.

[23] Cabrini M, Cigada A, Rondelli G, Vicentini B. Effect of different surface finishing and of hydroxyapatite coatings on passive and corrosion current of Ti6Al4V alloy in simulated physiological solution. Biomaterials 1997;18:783–7.

[24] Hayashi K, Noda I, Uenoyama K, Sugioka Y. Breakdown corrosion potential of ceramic coated metal implants. J Biomed Mater Res 1990;24:1111–3.

[25] Sousa SR, Barbosa MA. Effect of hydroxyapatite thickness on metal ion release from Ti6Al4V substrates. Biomaterials 1996;17:397–404.

[26] Sridhar TM, Kamachi Mudali U, Rajeswari S, Subbaiyan M. Electrochemical impedance studies on hydroxyapatite coated type 316L stainless steel. In: Proceedings of the 7th International Symposium on Electrochemical Methods in Corrosion Research. Budapest, 2000, Paper No. 110.

[27] Bard AJ, Faulkner LR. Electrochemical methods: fundamentals and applications, 2nd ed. New York: Wiley; 2001 [Chapter 10].

[28] Mansfeld F. Analysis, interpretation of EIS data for metals and alloys. Farnborough, Solartron-Schlumberger, 1993, Technical Report 26 [Chapter 4].

[29] Thompson I, Campbell D. Interpreting Nyquist responses from defective coatings on steel substrates. Corros Sci 1994;36:187–98.
[30] Baltat-Bazia A, Celati N, Keddam M, Takenouti H, Wiart R. Electrochemical impedance spectroscopy and electron microscopies applied to the structure of anodic oxide layer on pure aluminum. Mater Sci Forum 1992;111–112:359–68.
[31] Boukamp BA. Equivalent circuit, manual AC-immittance data analysis system. Enschede: Twente University of Technology; 1989.
[32] Bardwell JA, McKubre MCH. AC impedance spectroscopy of the anodic film on zirconium in neutral solution. Electrochim Acta 1991;36:647–53.
[33] Boukamp BA. A package for impedance/admittance data analysis. Solid State Ionics 1986;18:136–40.
[34] Pan J, Thierry D, Leygraf C. Electrochemical impedance spectroscopy study of the passive oxide film on titanium for implant application. Electrochim Acta 1996;41:1143–53.
[35] Pan J, Leygraf C, Thierry D, Ektessabi AM. Corrosion resistance for biomaterial applications of TiO_2 films deposited on titanium and stainless steel by ion-beam-assisted sputtering. J Biomed Mater Res 1997;35:309–18.
[36] Pan J, Thierry D, Leygraf C. Electrochemical and XPS atudies of titanium for biomaterial applications with respect to the effect of hydrogen peroxide. J Biomed Mater Res 1994;28:113–22.